

Hyperthermal Collisions of $O^+(^4S_{3/2})$ with Methane at 5 Electron Volts

Lipeng Sun* and George C. Schatz†
Northwestern University, Evanston, Illinois 60208

Preliminary studies were carried out for the $O^+(^4S_{3/2})$ + methane reaction, which serves as a benchmark for developing the theory of polymer erosion by O^+ under low Earth orbit conditions. Ab initio electronic structure calculations show that the interaction of O^+ with CH_4 can lead to a large number of reaction products such as charge transfer, hydride abstraction, and H elimination. Based on the information obtained from these quantum chemistry calculations, a direct dynamics classical trajectory simulation was carried out at 5-eV relative translation energy and the chemical reaction channels predicted by the ab initio calculations are confirmed.

I. Introduction

WHEN space vehicles travel in low Earth orbit (LEO) or geosynchronous Earth orbit (GEO), their surfaces are under constant bombardment by energetic atoms/molecules, ions, electrons and various sources of electromagnetic radiation. Among these collision processes, atomic/molecular ions are responsible for space vehicle charging and atmospheric drag. In the LEO and GEO environments, ions may have kinetic energies ranging from 1 to 10^6 eV (Refs. 1 and 2). As a consequence, various chemical processes that carry mass away from the surfaces can be induced and enhanced due to ion/surface collisions that cause chemical reaction, energy transfer and surface ionization. Therefore, it is important to understand ion/surface erosion mechanisms at the microscopic level and to evaluate the relative importance of ions compared to neutrals (such as atomic oxygen) in producing erosion. Although there have been extensive studies of $O(^3P)$ erosion mechanisms on the surfaces of spacecraft,^{3,4} surprisingly, the microscopic reaction mechanisms of the $O^+(^4S)$ ion, the most abundant ionic species in LEO (with a LEO abundance that is roughly 10^{-4} of the O abundance), are mostly unknown.⁵ Recent experimental work has been carried out for the reaction of O^+ with small alkane molecules in the gas phase using the guided-ion beam time-of-flight technique⁶ and for O^+ reacting with decanethiolate/Au(111) self-assembled monolayers.^{7,8} These experiments provide important details concerning reaction mechanisms, but leave open a number of important questions, including the following: 1) What is the relationship between charge transfer (the most important process when O^+ interacts with organics) and reaction? 2) What is the relationship between the gas phase experiments, in which a broad range of positive ions (OH^+ , H_2O^+ , CH_3O^+ , H_2CO^+ , HCO^+ , CO^+ , CH_2^+ , CH_3^+ , CH_4^+) are produced, and the gas/surface experiments, in which a few negative ions (O^- , OH^-) dominate the ion yield? 3) Is the relative efficiency of O^+ compared to O in the degradation of polymers such that O^+ can play an important role in degradation despite its lower abundance? 4) Is O^+ degradation similar enough to O degradation so that one can use O^+ gas/surface experiments to learn about O degradation? Answering these questions is going to be difficult, but it will be significantly aided if we have good theoretical models of the O^+ reaction dynamics. However, extensive theoretical characterization of these reaction systems was not done until very recently.^{9,10}

In an attempt to develop theory that will assist in answering these questions, in this paper we report both ab initio electronic structure theory and classical trajectory simulations of the $O^+ + CH_4$ reaction mechanisms and dynamics. Although the focus of this work is on the gas-phase dynamics, this study will provide detailed information about the formation/cleavage of C–O, O–H, C–H, and H–H bonds, which should be useful for understanding the closely related polymer erosion mechanisms in O^+ /surface collisions. In addition, this work will establish the level of theory needed to study the more complicated gas/surface processes.

II. Results

A. Ab Initio Calculations

In the LEO environment, the kinetic energy of O^+ is about 5 eV relative to the traveling space vehicle. With this energy, a large number of reactions are energetically accessible. To evaluate the reaction energies, ab initio electronic structure calculations were performed using the quantum chemistry software package GAMESS.¹¹ The calculated structures and energies are shown in Fig. 1. It turns out that second-order perturbation theory with a modest basis set, MP2/6-31G**, gives reasonable energetics and geometries. The 0-K heats of reaction calculated with MP2/6-31G** for the energetically accessible reaction channels show a mean absolute deviation compared with available experiments¹² of 0.35 eV, which is acceptable given the 5-eV available energy.

Charge transfer can be viewed as a simple type of chemical reaction in which one or several electrons move from one chemical species to another. For the $[O\cdots CH_4]^+$ system, charge transfer, $O^+ + CH_4 \rightarrow CH_4^+ + O$, is exothermic and can be described by a near-resonant electron-transfer mechanism. In this scenario, charge transfer occurs at primarily large impact parameters with negligible momentum transfer between the colliding species. The recently measured experimental charge-transfer cross section supports this picture.⁹ The large charge-transfer cross section (about 80 \AA^2) allows us to model the subsequent chemical processes by studying the $O + CH_4^+$ collision system. The equilibrium structures of the charge transfer intermediate CH_4^+ have been extensively studied in the past 20 years.^{13–16} Its symmetry, due to Jahn–Teller effects, is reduced from T_d to C_{2v} , D_{2d} , and C_{3v} , with C_{2v} as its most stable structure, as depicted in Fig. 1.

After charge transfer, many processes can take place in the several accessible electronic states. In the lowest quartet electronic state, the primary products that are thermodynamically favorable are found to be $CH_3 + OH^+$, $H_2CO^+ + 2H$, $H_2O^+ + CH_2$, and $CH_3O^+ + H$. All of these reactions are exothermic. In addition, when O approaches the CH_4^+ ion a reaction intermediate is formed, and the stable structure due to the ion–molecule electrostatic interaction, as shown in Fig. 1, is the configuration formed when O approaches the vertex of CH_4^+ . The CH_4 moiety of the reaction intermediate is very close to the C_{3v} symmetry of CH_4^+ with the charge located on the

Received 24 January 2005; revision received 26 July 2005; accepted for publication 10 September 2005. Copyright © 2005 by the American Institute of Aeronautics and Astronautics, Inc. All rights reserved. Copies of this paper may be made for personal or internal use, on condition that the copier pay the \$10.00 per-copy fee to the Copyright Clearance Center, Inc., 222 Rosewood Drive, Danvers, MA 01923; include the code 0022-4650/06 \$10.00 in correspondence with the CCC.

*Postdoctoral Fellow, Department of Chemistry; lpsun@chem.northwestern.edu.

†Professor of Chemistry, Department of Chemistry; schatz@chem.northwestern.edu.

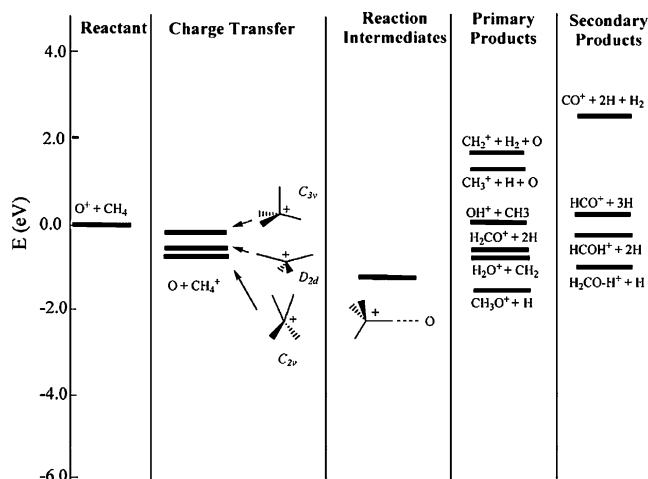


Fig. 1 Energy diagram for $\text{O}^+ + \text{CH}_4$. Energies were calculated at MP2/6-31G** level of theory.

CH_4 moiety. It is interesting to notice that there is no reaction barrier for $[\text{H}_3\text{CH}-\text{O}]^+ \rightarrow \text{CH}_3 + \text{OH}^+$, which indicates that direct dissociation should readily occur. With such a strong electrostatic interaction (-1.01 eV) between CH_4^+ and O, a complex-mediated reaction mechanism is expected in which O and CH_4^+ first form the $[\text{H}_3\text{CH}-\text{O}]^+$ complex and then this is trapped in a deep potential energy well for a certain period of time. Subsequently this either directly dissociates to $\text{OH}^+ + \text{CH}_3$ or undergoes further chemical reactions such as $\text{OH}^+ + \text{CH}_3 \rightarrow \text{CH}_2 + \text{H}_2\text{O}^+$. These mechanisms should be especially important for low collision energies at which all these exothermic reactions are expected to occur. With increased collision energy, however, this complex-mediated mechanism becomes less and less important. Instead, a direct reaction mechanism becomes more important. For example, for the $[\text{H}_3\text{CH}-\text{O}]^+ \rightarrow \text{CH}_3 + \text{OH}^+$ reaction, the incoming O atom can directly grab one H atom from CH_4^+ without exchanging much of its kinetic energy. This mechanism is usually referred as a stripping mechanism. There are also endothermic reactions, such as $\text{CH}_3^+ + \text{H} + \text{O}$ and $\text{CH}_2^+ + \text{H}_2 + \text{O}$, possible on the quartet potential energy surface. Because the available energy for the reaction (5 eV) is much larger than the dissociation threshold (0.8 eV for $\text{CH}_4^+ \rightarrow \text{CH}_3^+ + \text{H}$ and 1.7 eV for $\text{CH}_4^+ \rightarrow \text{CH}_2^+ + \text{H}_2$), these reactions can occur with a collision-induced dissociation (CID) mechanism in which the CH_4^+ cation receives enough internal energy from the collision with O to dissociate into $\text{CH}_3^+ + \text{H}$ or $\text{CH}_2^+ + \text{H}_2$.

The $\text{O}^+ + \text{CH}_4$ reaction can also occur on doublet surfaces that are accessible from the initial quartet surface via intersystem crossing. The doublet surfaces generally give products that are more exothermic than their quartet counterparts, so spin-forbidden reaction mechanisms could be important, in spite of the fact that the spin-orbit coupling in this system is weak. However, our recent calculations show that the reaction cross sections obtained using quartet-only trajectories are in good agreement with experiment for energies above 1 eV (Ref. 8). Thus at least at high energies, at which direct mechanisms should be dominant, intersystem crossing is apparently not very important. At low energies, where reaction through a complex should dominate and there are more opportunities for accessing the quartet/doublet crossing seams, it is possible that the reactions on the doublet surface play a role. In the present work we ignore spin-forbidden processes.

Because a majority of the energetically accessible reaction channels are exothermic, at high impact energies, the primary products such as CH_3O^+ and H_2CO^+ can further isomerize to $\text{H}_2\text{C}-\text{OH}^+$ and $\text{HC}-\text{OH}^+$ or dissociate directly to HCO^+ . In addition, $\text{H}_2\text{C}-\text{OH}^+$, $\text{HC}-\text{OH}^+$, and HCO^+ may further dissociate to CO^+ product. These products are also shown in Fig. 1.

B. Direct Dynamics Simulation

Energetics calculations in the preceding section provide qualitative information about which reactions can occur, but quantitative

information about the reaction dynamics can be revealed only by performing dynamics simulations. To provide a further understanding of the $[\text{O} \cdot \text{CH}_4]^+$ reaction dynamics, direct dynamics classical trajectory simulations were performed in which the energy gradient was obtained directly from a semiempirical Hamiltonian (PM3) on the quartet potential energy surface.¹⁷ Although the mean absolute deviation between PM3 and MP2 is 0.45 eV (Ref. 10), it can provide accuracy that is adequate at 5 eV collision energy, as shown in the following results. In fact, at higher energies, even better agreement can be achieved.¹⁰ Trajectory initial conditions were chosen by a quasi-classical sampling method for the CH_4^+ . The colliding O atom has a translational energy of 5 eV relative to CH_4^+ . The reactive trajectories were integrated for 500 fs to monitor secondary monomolecular dissociation processes. This means that slower secondary chemistry than this is not included, so the yields of less stable ions, such as H_2CO^+ , must be regarded as upper bounds to what would be seen in experiment. The products found from the simulation and their branching fractions are shown in Table 1. Many reaction products, especially the oxygenated species, are found. Snapshots of several representative trajectories are depicted in Fig. 2 for illustration.

All the possible products predicted by the quantum chemistry calculations are found in the trajectory simulation. The reactants proceed to products within a few hundred femtoseconds, so long-lived

Table 1 Reaction products, branching fractions, and their cross sections^a

Product	Branching fraction	Cross section (\AA^2)
$\text{OH}^+ + \text{CH}_3$	12.4%	1.67 (± 0.15)
$\text{CH}_3^+ + \text{H} + \text{O}$	7.0%	0.94 (± 0.11)
$\text{CH}_3^+ + \text{OH}$	12.4%	1.66 (± 0.14)
$\text{HCO}^+ + 3\text{H}$	29.5%	3.97 (± 0.22)
$\text{H}_2\text{CO}^+ + 2\text{H}$	2.3%	0.32 (± 0.07)
$\text{CH}_2^+ + \text{H}_2 + \text{O}$	24.8%	3.35 (± 0.20)
$\text{H}_2\text{O}^+ + \text{CH}_2$	6.2%	0.83 (± 0.1)
$\text{CO}^+ + \text{H}_2 + 2\text{H}$	5.4%	0.73 (± 0.1)
Other	< 1%	< 0.14

^aResults are based on PM3 calculations on the lowest potential-energy surface.

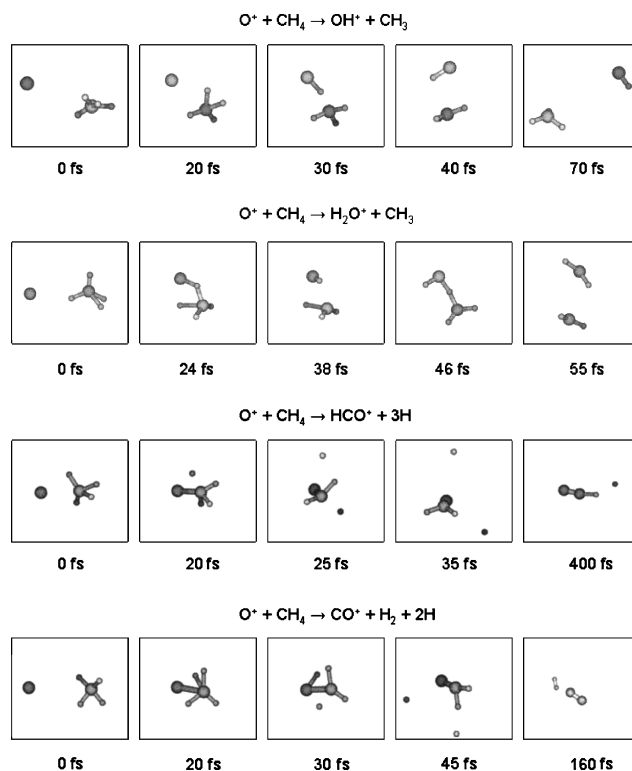


Fig. 2 Snapshots of four reactive trajectories for OH^+ , H_2O^+ , HCO^+ , and CO^+ ionic products.

complexes are not important. The $\text{CH}_3^+ + \text{H} + \text{O}$ and $\text{CH}_2^+ + \text{H}_2 + \text{O}$ products are the result of a collision-induced dissociation reaction mechanism. The appearance of $\text{CH}_3 + \text{OH}^+$ is in agreement with the expected stripping mechanism (as shown in Fig. 2) on the quartet potential energy surface. As illustrated in Fig. 2, H_2O^+ is formed, at a collision energy of 5 eV, from a direct double-pickup mechanism. Both of the $\text{CH}_3^+ + \text{OH}^+$ and $\text{H}_2\text{O}^+ + \text{CH}_2^+$ reactions are direct processes, as clearly shown in Fig. 2. This is in contrast to their reaction mechanisms at low collision energies.¹⁰ HCO^+ is a secondary product that comes from H_2CO^+ . The small fractional population of the H_2CO^+ cation radical indicates that when it is formed the energy transferred to H_2CO^+ is sufficient for its dissociation. For the particular trajectory shown in Fig. 2, it takes several rotational periods for H_2CO^+ to dissociate, whereas the dissociation of the first two C–H bonds happens very fast and almost simultaneously. Therefore, at 5 eV, it is often hard to distinguish the primary and secondary reactions due to rapid energy transfer. Similarly, this is also observed in the $\text{O}(^3\text{P}) + \text{ethane}$ reaction.¹⁸ Interestingly, a CO^+ product is also found with a nonnegligible branching fraction. The multistep mechanism in Fig. 2 for the CO^+ trajectory indicates that there exist complex microscopic reaction pathways for its formation. Comparison of the cross sections in Table 1 with experiment has been discussed in our earlier work,¹⁰ where it was noted that the cross sections for families of products, such as $\text{CH}_3^+ + \text{CH}_2^+$ and $\text{H}_2\text{CO}^+ + \text{HCO}^+ + \text{CO}^+$, agree with experiment semiquantitatively, but some of the individual results do not, due to inaccuracies in the potential surface. For example, experimental cross sections for CH_3^+ and CH_2^+ are about 7.5 and 0.7 Å², whereas the trajectory calculation gives 2.6 and 3.4 Å², respectively. For other ions such as HCO^+ , H_2O^+ , and H_2CO^+ the difference is much smaller (~ 0.2 Å²).

III. Conclusions

Overall, quantum chemistry calculations and classical trajectory simulations have shown that the reaction of O^+ and CH_4 is efficient at a collision energy of 5 eV. The total cross section for the reactive channels is about 13.5 Å². Many reaction products were found on the quartet potential energy surfaces. Charge transfer happens via a quasi-resonant mechanism at large impact parameter and is the dominant process. Chemical reactions including the formation of C–O and O–H bonds occur at smaller impact parameters, and we have interpreted these results by an intermediate-mediated reaction mechanism at low collision energy and a collision-induced dissociation/direct reaction mechanism at high impact energy. Because of the low energy barriers and large exothermicity of these reaction channels, subsequent secondary reactions involving unimolecular dissociation mechanisms are also efficient. This is in contrast to the $\text{O} + \text{CH}_4$ reaction.³ This may suggest that for O^+ colliding with surface materials (e.g., alkylthiolate self-assembled monolayer surface), volatile products such as H_2CO^+ , HCO^+ , and CO^+ from the degradation of the RO^+ cation radical may also be more efficient than those from the O reaction.

Perhaps the most important conclusion from this work is that it is possible to use direct dynamics simulation with the PM3 semiempirical method to provide a semiquantitative description of the high-energy dynamics of O^+ interacting with methane. With this understanding, our future work will focus on O^+ reactions with alkyl thiol self-assembled monolayer surfaces and other types of material surfaces.

Acknowledgments

This research was supported by Air Force Office of Scientific Research Multidisciplinary University Research Initiative Grant

F49620-01-1-0335. This paper is based on work presented at the International Conference on Protection of Materials and Spacecraft from Space Environment-7 (ICPMSE-7), Toronto, 10–14 May 2004.

References

- Dressler, R. A., and Murad, E., "The Gas-Phase Chemical Dynamics Associated with Meteors," *Chemical Dynamics in Extreme Environments*, edited by R. A. Dressler, World Scientific, Singapore, 2001, pp. 268–348.
- Jacobs, D. C., "Dynamics of Hypervelocity Gas/Surface Collisions," *Chemical Dynamics in Extreme Environments*, edited by R. A. Dressler, World Scientific, Singapore, 2001, pp. 349–389.
- Troya, D., and Schatz, G. C., "Hyperthermal Chemistry in the Gas Phase and on Surfaces: Theoretical Studies," *International Reviews in Physical Chemistry*, Vol. 23, No. 3, 2004, pp. 341–373.
- Minton, T. K., and Garton, D. J., "Dynamics of Atomic Oxygen Induced Polymer Degradation in Low Earth Orbit," *Chemical Dynamics in Extreme Environments*, edited by R. A. Dressler, World Scientific, Singapore, 2001, pp. 420–489, and references therein.
- Lyubimova, G. V., and Shestakov, A. F., "A Theoretical Study of Pathways of the O^+ with Methane," *Kinetics and Catalysis*, Vol. 35, No. 2, 1994, pp. 208–212.
- Levandier, D. J., Chiu, Y. H., and Dressler, R. A., "Reactions of O^+ with $\text{C}_n\text{H}_{2n+2}$, $n = 2-4$: A Guided Ion-Beam Study," *Journal of Chemical Physics*, Vol. 120, No. 15, 2004, pp. 6999–7007.
- Qin, X., Tzvetkov, T., and Jacobs, D. C., "Reaction of 5 eV O^+ with a Decanethiolate/Au{111} Self-Assembled Monolayer," *Nuclear Instruments and Methods in Physics Research, Section B: Beam Interactions with Materials and Atoms*, Vol. 203, April 2003, pp. 130–135.
- Qin, X., Tzvetkov, T., Lin, X., Lee, D. C., Yu, L., and Jacobs, D. C., "Site-Selective Abstraction in the Reaction of 5–20 eV O^+ with a Self-Assembled Monolayer," *Journal of the American Chemical Society*, Vol. 126, No. 41, 2004, pp. 13,232–13,233.
- Levandier, D. J., Chiu, Y. H., Dressler, R. A., Sun, L., and Schatz, G. C., "Hyperthermal Reactions of $\text{O}^+(^4\text{S}_{3/2})$ with CD_4 and CH_4 : Theory and Experiment," *Journal of Physical Chemistry A*, Vol. 108, No. 45, 2004, pp. 9794–9804.
- Sun, L., and Schatz, G. C., "Direct Dynamics Classical Trajectory Simulations of $\text{O}^+ + \text{CH}_4$ Reaction at Hyperthermal Energies," *Journal of Physical Chemistry B*, Vol. 109, No. 17, 2005, pp. 8431–8438.
- Schmidt, M. W., Baldridge, K. K., Boatz, J. A., Elbert, S. T., Gordon, M. S., Jensen, J. H., Koseki, S., Matsunaga, N., Nguyen, K. A., Su, S. J., Windus, T. L., Dupuis, M., and Montgomery, J. A., "General Atomic and Molecular Electronic Structure System," *Journal of Computational Chemistry*, Vol. 14, No. 11, 1993, pp. 1347–1363.
- National Inst. of Standards and Technology, "Standard Reference Database 69," URL: <http://webbook.nist.gov> [cited June 2005].
- Paddonrow, M. N., Fox, D. J., Pople, J. A., Houk, K. N., and Pratt, D. W., "Dynamics Jahn–Teller Effects in CH_4^+ : Location of the Transition Structures for Hydrogen Scrambling and Inversion," *Journal of the American Chemical Society*, Vol. 107, No. 25, 1985, pp. 7696–7700.
- Frey, R. F., and Davison, E. R., "Potential Energy Surface of CH_4^+ ," *Journal of Chemical Physics*, Vol. 88, No. 3, 1988, pp. 1775–1785.
- Wetmore, S. D., Boyd, R. J., Eriksson, L. A., and Laaksonen, A., "A Combined Quantum Mechanics and Molecular Dynamics of Small Jahn–Teller Distorted Hydrocarbons: Another Difficult Test for Density Functional Theory," *Journal of Chemical Physics*, Vol. 110, No. 24, 1999, pp. 12,059–12,069.
- Signorelli, R., and Merkt, F., "The First Rotationally Resolved Spectrum of CH_4^+ ," *Journal of Chemical Physics*, Vol. 110, No. 5, 1999, pp. 2309–2740.
- Stewart, J. J. P., "Optimization of Parameters for Semiempirical Methods. I. Methods," *Journal of Computational Chemistry*, Vol. 10, No. 2, 1989, pp. 209–220.
- Yan, T., Doubleday, C. J., and Hase, W. L., "A PM3-SRP Plus Analytic Function Potential Energy Surface Model for $\text{O}(^3\text{P})$ Reactions with Alkanes. Application to $\text{O}(^3\text{P}) + \text{Ethane}$," *Journal of Physical Chemistry A*, Vol. 108, No. 45, 2004, pp. 9863–9875.

J. Kleiman
Guest Editor